Absence of Two-Dimensional Bragg Glasses

Chen Zeng,[1] P. L. Leath,[1] and Daniel S. Fisher[2]
[1]*Department of Physics and Astronomy, Rutgers University, Piscataway, New Jersey 08854*
[2]*Department of Physics, Harvard University, Cambridge, Massachusetts 02138*
(Received 20 July 1998)

The stability to dislocations of the elastic phase, or "Bragg glass," of a randomly pinned elastic medium in two dimensions is studied using the minimum-cost-flow algorithm for a disordered fully packed loop model. The elastic phase is found to be unstable to dislocations due to the quenched disorder. The energetics of dislocations are discussed within the framework of renormalization group predictions as well as in terms of a domain wall picture. [S0031-9007(99)08587-7]

PACS numbers: 74.60.Ge, 02.60.Pn, 64.70.Pf

Randomly pinned elastic media are used to model various condensed-matter systems with quenched disorder, including flux-line arrays in dirty type-II superconductors [1] and charge density waves (CDW) [2]. Although it is known [3] that these systems cannot exhibit long-range translational order in less than four dimensions, the intriguing possibility of a "topologically ordered" low-temperature phase remains an open question [1,4,5]. It has been conjectured that such a phase, with all dislocation loops bound, exists in three dimensions. Such a phase would be elastic and have power-law Bragg-like singularities in its structure factor; it is often referred to as a "Bragg" or "elastic" glass [4].

Whether or not unbound topological defects exist at low temperatures involves a subtle balance between elastic-energy cost and disorder-energy gain [5]. We analyze this issue for two-dimensional randomly pinned elastic media at zero temperature by considering a $2d$-lattice model, viz., a fully packed loop (FPL) model [6] with quenched disorder. This FPL model is equivalent to an array of planar fluxlines [7], a prototypical model for elastic media. Exact ground states of the FPL model are computed with and without topological defects, which we refer to as dislocations. The *polynomial* optimization algorithm [8] that we use, minimum-cost-flow, enables us to study large systems.

We focus on the energetics of a single dislocation pair in systems of size $L \times L$. Our main conclusion is that the disorder energy gain of the optimally placed pair dominates over the elastic energy cost with the results being consistent with theoretical predictions of $O(-(\ln L)^{3/2})$ and $O(+\ln L)$, respectively, for the two quantities. Dislocations therefore become unbound and proliferate causing the destruction of the Bragg glass in the thermodynamic limit [9].

Model and algorithm.—The FPL model is defined on a honeycomb lattice on which all configurations of occupied bonds which form closed loops and cover every site exactly once are allowed, as shown in Fig. 1(a). This model can be mapped to a solid-on-solid surface model. Define integer heights at the centers of hexagons then orient all bonds of the resulting triangular lattice such that elementary triangles pointing upward are circled clockwise; assign $+1$ to the difference of neighboring heights along the oriented bonds if a loop is crossed and -2 otherwise. This yields single-valued heights up to an overall constant. It can be seen that the smallest "step" of the surface is three, so that the effective potential on the surface is periodic in heights modulo 3.

Quenched disorder is introduced via random bond weights on the honeycomb lattice, chosen independently and uniformly from integers in the interval $[-500, 500]$. The energy is the sum of the bond weights along all loops and strings. The system can be viewed as a surface in a $3d$ random medium that is periodic in the height direction. Dislocations are added to the FPL model by "violating" the constraint. One dislocation pair is an open string in an otherwise fully packed system as shown in Fig. 1(b). The height change along any path encircling one end of the string is the Burgers charge ± 3 of a dislocation so that the heights become multivalued.

Numerical results.—For each disorder realization, the ground-state energies with and without a dislocation pair and hence the defect energy E_d and also the domain wall [see Fig. 1(c)] were computed by an integer min-cost-flow algorithm [8].

We first held the dislocations *fixed* at two specific sites separated by $L/2$ in $L \times L$ samples with $L = 12$,

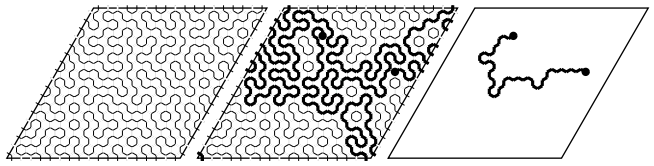

FIG. 1. The FPL model with periodic boundary conditions. The ground states with and without a pair of dislocations for one realization of random bond weights are displayed in (b) and (a), respectively. The dislocations (solid dots) in (b) are connected by an open string (thick line) among the loops. The relevant physical object is, however, the dislocation-induced domain wall, as shown in (c). This domain wall represents the line of bond *differences* between the ground states (a) and (b).

24, 48, 96, 192, and 384, with at least 10^4 disorder realizations for each size. The probability distributions $P(E_d)$ of the defect energy are shown in Fig. 2(a); they are well fit by Gaussians for all sizes. The mean pair energy is plotted versus $\ln L$ with a linear fit $\overline{E}_d = 180(2)\ln L - 20(6)$. The root-mean-square (rms) width $\sigma(E_d)$ is also shown in Fig. 2(b), with a linear fit of $\sigma(E_d) = 250(3) + 133(1)\ln L$. This implies a tail in $P(E_d)$ for negative E_d and suggests an energy *gain* from dislocations that can be optimized to take advantage of the negative part of the distribution.

We also computed the *optimized* (lowest energy) dislocation pair energy $E_d^{\min}$ for L up to 480 with 10^4–10^6 samples for each size. The defect energy distribution $P(E_d^{\min})$ is no longer Gaussian, indeed substantial asymmetry in $P(E_d^{\min})$ is seen in Fig. 3(a). Moreover, in contrast to the case of fixed dislocations, $\overline{E}_d^{\min}$ is *negative* and *decreases* more rapidly than $\ln L$ with increasing system size while the rms width $\sigma(E_d^{\min})$ increases less rapidly than $\ln L$. The linear fits shown in Fig. 3(b) yield $[-\overline{E}_d^{\min}]^{2/3} = (43.80 \pm 0.31)\ln L + (24.03 \pm 0.14)$ and $[\sigma(E_d^{\min})]^2 = (21883 \pm 180)\ln L + (9013 \pm 802)$. This implies that since almost all large systems have negative energy dislocation pairs, as is evident in Fig. 3(a), the FPL model is *unstable* against the spontaneous appearance of dislocations.

Continuum models.—To understand analytically the observed defect energetics, we consider coarse-grained approximations to the random FPL model. In the absence of dislocations, the surface has a stiffness caused by the inability of a tilted surface to take as much advantage of the low weight bonds as a flatter surface. The random bonds couple to both ∇h and h modulo $b = 3$. An appropriate effective Hamiltonian is thus

$$H = \int d\mathbf{r}\left[\frac{K}{2}(\nabla h)^2 - \mathbf{f}\cdot\nabla h - w\cos\left(\frac{2\pi}{3}h - \gamma\right)\right], \tag{1}$$

with $\mathbf{f} \equiv \mathbf{f}(\mathbf{r})$ locally random with variance Δ, and $\gamma \equiv \gamma(\mathbf{r}) = 0, \pm\frac{2\pi}{3}$ with equal probability.

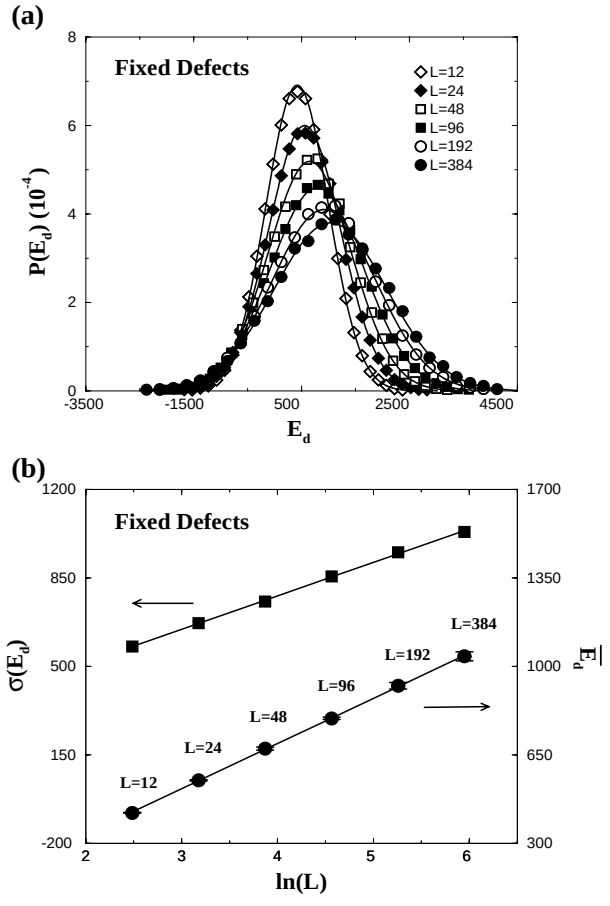

FIG. 2. Energetics of *fixed* defects: The probability distributions of the energy of a *fixed* dislocation pair with separation $L/2$ for sample sizes from $L = 12$ to $L = 384$ are shown in (a). The solid lines are Gaussian fits. The corresponding average defect energy $\overline{E}_d$ (solid circle) and the rms width $\sigma(E_d)$ (solid square) are found to scale with system size as $\ln L$, as shown in (b). The solid lines are linear fits.

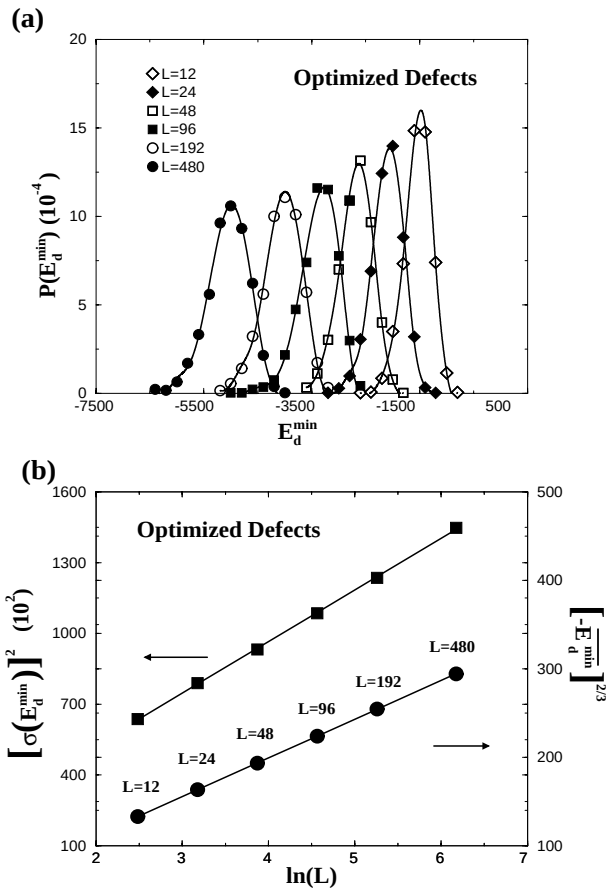

FIG. 3. Energetics of *optimized* defects: The defect energy probability distributions for sample sizes from $L = 12$ to $L = 480$ are shown in (a). The solid lines are guides to the eyes. Both the average defect energy plotted as $[-\overline{E}_d^{\min}]^{2/3}$ vs $\ln L$ and the rms width plotted as $[\sigma(E_d^{\min})]^2$ vs $\ln L$ are shown in (b). Solid lines are linear fits.

A related model (CDW) [10] has, instead, the $\{\gamma(\mathbf{r})\}$ being uniformly distributed in $[0, 2\pi]$. A renormalization group (RG) analysis [11] shows that these models are in the same universality class: shifting $h(\mathbf{r})$ by $\frac{3}{2\pi}\gamma(\mathbf{r})$ makes the models similar but changes the $\{f(\mathbf{r})\}$ introducing short-range correlations that are different in the two models. However, these are irrelevant on large length scales since the variations of h grow without bound.

The CDW model has an elastic glass phase for $T < T_g$ in which w is relevant and renormalizes to a T-dependent fixed point while Δ grows as $\ln L$ yielding height variations $\overline{\langle[h(\mathbf{r}) - h(0)]^2\rangle} \approx \frac{b^2}{\pi}\Upsilon(\ln r)^2$ [10]. An approximate functional RG analysis yields a similar structure at all temperatures below T_g with a universal $T = 0$ limit Υ_0 of the coefficient $\Upsilon(T)$ [12]. On large scales, the behavior is dominated by the competition between the random stressing $\mathbf{f}(\mathbf{r})$, and the stiffness K, with the random force correlations effectively $\overline{f_i(\mathbf{q})f_j(-\mathbf{q})} = -C\delta_{ij}\ln(q^2)$ for small wave vectors q. We can thus work with the simple purely random-force limit of Eq. (1) with $w = 0$. We then immediately conclude that $\Upsilon_0 = \frac{C}{K^2b^2}$.

In the presence of dislocations $h(\mathbf{r})$ becomes multivalued. It can be decomposed into two parts $h = h_e + h_d$, with h_e, the smooth elastic distortion while the singular function h_d, has a cut connecting the two dislocations at $\mathbf{r}_1$ and $\mathbf{r}_2$ with Burgers charge $b_1 = b = 3$ and $b_2 = -b = -3$ with $\nabla \times \nabla h_d = \sum_{i=1,2} b_i \delta^2(\mathbf{r} - \mathbf{r}_i)$ and $\nabla^2 h_d = 0$. The energy of a dislocation pair is

$$E_d = \frac{K}{2}\int d^2\mathbf{r}|\nabla h_d|^2 - \int d^2\mathbf{r}(\mathbf{f}^T \cdot \nabla h_d) \quad (2)$$

$$\approx \frac{Kb^2}{2\pi}\ln|\mathbf{r}_1 - \mathbf{r}_2| - b[g(\mathbf{r}_1) - g(\mathbf{r}_2)], \quad (3)$$

where the static random force field has been decomposed into longitudinal $\mathbf{f}^L = \nabla u(\mathbf{r})$ and transverse $\mathbf{f}^T = \nabla \times g(\mathbf{r})$ components. Since $u(\mathbf{r})$, $g(\mathbf{r})$, and ∇h_d are continuous across the cut while h_d jumps by b, $\mathbf{f}^L$ makes no contribution to E_d and Eq. (3) follows by integration by parts. The first term is the standard elastic cost and the second the disorder gain so that $g(\mathbf{r})$ is the *potential* felt by the dislocations. Its variance is $S_g \equiv \overline{g(\mathbf{q})g(-\mathbf{q})} = -Cq^{-2}\ln(q^2)$ so that the elastic surface without dislocations and the dislocation potential have the *same statistics* after a rescaling: $S_h \equiv \overline{h(\mathbf{q})h(-\mathbf{q})} \approx S_g/K^2$.

In terms of the statistical properties of the dislocation potential, our numerical results can be understood. We first discuss fixed dislocation pairs. A statistical symmetry of the CDW model implies that on large scales $f(\mathbf{r})$ and hence the potential $g(\mathbf{r})$ and E_d are Gaussian [12]. The shape of our computed defect energy distribution, its mean, and its variance all agree with predictions from Eq. (3), $\overline{E}_d \approx (Kb^2/2\pi)\ln L$—an exact result for the CDW model—and $\sigma(E_d) \approx \sqrt{b^2C/\pi}\ln L$ with $K = 126(2)$ and $C = 6174(93)$ yielding $C/K^2 = 0.389(11)$. We also measured the variance of the height of the surface without dislocations, finding a good fit to $\sigma^2(h) = 0.061(2)(\ln L)^2 + 0.477(7)\ln L + 0.765(13)$. The predicted coefficient of the $(\ln L)^2$ is $C/2\pi K^2$ yielding $C/K^2 = 0.387(12)$. The agreement between the two estimates of C/K^2 further supports the validity of the random force model, including, in particular, the equality between the statistics of the longitudinal and transverse parts of $\mathbf{f}(\mathbf{r})$

We now turn to optimized dislocations. If the first term in Eq. (3) can be ignored, the optimal placement of dislocations coincides with the minimum ($g_{\min}$) and maximum ($g_{\max}$) of the random potential $g(\mathbf{r})$. The distribution of the extrema of potentials like $g(\mathbf{r})$, whose variance grows as a power of $\ln L$, can be semiquantitatively understood by thinking of iteratively optimizing over each factor of 2 in length scale with the component of the random potential on scale l being essentially the contribution from Fourier components with $(\sqrt{2}\,\pi/l) < |q_x|, |q_y| < (2\sqrt{2}\,\pi/l)$. If scale l gives rise to a contribution to the variance of g of order $(\ln l)^{2\alpha}$—with $\alpha = \frac{1}{2}$ in our case—then a *typical* $g(\mathbf{r})$ is the incoherent logarithmic sum over all scales, i.e., $\sim(\ln l)^{\alpha+1/2}$. The maximum of g can be found, heuristically, by maximizing over the four points at scale $l = 1$ in each square of scale-2, then maximizing over the four scale-2 maxima in each scale-4 square, etc. Since the scale l structure of g is weakly correlated over scales much longer than l, a crude approximation is to ignore these correlations whereby one stage of optimization adds of order $(\ln l)^\alpha$ to the local scale l maximum [13]. Thus scales should be summed over *coherently* yielding $g_{\max} \sim (\ln L)^{\alpha+1}$. The variance of $g_{\max}$ is dominated by the largest scales, so that $\sigma(g_{\max}) \sim (\ln L)^\alpha$. In our case, we thus expect $\overline{g_{\max} - g_{\min}} \sim (\ln L)^{3/2}$ which indeed dominates over the $\ln L$ elastic energy term in Eq. (3). Hence we expect $\overline{E}_d^{\min} \approx -Ab\sqrt{C}(\ln L)^{3/2}$ and $\sigma(E_d^{\min}) \approx Bb\sqrt{C}(\ln L)^{1/2}$ with some coefficients A and B.

The linear fits in Fig. 3(b) give $A \approx 1.23(1)$ and $B \approx 0.56(1)$ using the C computed earlier. If the elastic part $\frac{Kb^2}{2\pi}\ln L$ is subtracted from $\overline{E}_d^{\min}$ by fitting the difference $\overline{E_d^{\min}(L)} - \overline{E_d^{\min}(L/2)}$ to $-(3\ln 2/2)Ab\sqrt{C}(\ln L)^{1/2} + \text{const}$, this yields a similar value of $A \approx 1.17(5)$. Using the extremal heights in the absence of dislocations, the stiffness K can also be extracted from $E_d^{\min}(L)$ via $\overline{E}_d^{\min} - bK\overline{(h_{\min} - h_{\max})} \approx \frac{Kb^2}{2\pi}\ln L + \text{const}$. This yields $K \approx 114(1)$ in not unreasonable agreement with the $K \approx 126(2)$ from the *fixed* dislocation pairs.

An upper bound on $\overline{g_{\max} - g_{\min}}$ can be simply obtained by noting that the probability $\text{Prob}[g_{\max} > M] \le \sum_{\mathbf{r}} \text{Prob}[g(\mathbf{r}) > M]$ so that, with L^2 points, the median $g_{\max}$ is less than the M for which the right-hand side, $L^2\,\text{Prob}[g(\mathbf{r}) > M]$ for fixed $\mathbf{r}$, equals $\frac{1}{2}$. If $g(\mathbf{r})$ is Gaussian sufficiently far into the tail of its distribution, this yields $\overline{g_{\max} - g_{\min}} \le \sqrt{C}\sqrt{8/\pi}\,(\ln L)^{3/2}$ so that $A \le \sqrt{8/\pi}$. The hierarchical optimization described

above suggests that A might saturate this bound [14]. To test this and the universality of A, we have measured the distributions of the extrema of the heights of the FPL surface without dislocations and several exactly Gaussian random surfaces $\{s(r)\}$ with variance $\overline{[s(r)]^2} = \frac{C}{2\pi}(\ln L)^{1+2\alpha}$. Good fits are found to $A\sqrt{C}\,(\ln(L/a_\alpha))^{1+\alpha}$ with a_α a cutoff, yielding $A_{\text{FPL-heights}} \approx 1.45(3)$, and $A_{\text{Gaussian}} \approx 1.517(3)$, 1.307(6), 1.168(6), and 1.064(5) for $\alpha = 0$, $1/2$, 1, and $3/2$, respectively, and from the variances $B_{\text{FPL-heights}} \approx 0.67(2)$, and $B_{\text{Gaussian}} \approx 0.475(4)$, 0.637(7), 0.730(9), and 0.814(4), respectively.

All the extracted A's satisfy $A \leq \sqrt{8/\pi}$, and there appears to be a systematic trend for $A(\alpha)$ to decrease as α increases; if so, it is likely that A is strictly less than $\sqrt{8/\pi}$ for all $\alpha > -\frac{1}{2}$ [for $\alpha < -\frac{1}{2}$ Gaussian surfaces the variance saturates for large L and the extrema grow as $(\ln L)^{1/2}$]. The values of A for the nominally $\alpha = \frac{1}{2}$ cases, 1.17–1.23, 1.45, and 1.307 for the optimal dislocations, extrema heights, and Gaussian surface, respectively, differ by substantially more than the apparent statistical errors as do the B's, 0.56, 0.67, and 0.637, respectively. But given the narrow range of $\ln L$ available, these results are certainly consistent with universal values of A and B for $\alpha = \frac{1}{2}$. The questions of universality and possible α dependence need further study.

Overall, we have found rather good agreement for a variety of large scale quantities with the RG prediction of equivalence at long scales of the FPL model and a random force model. Although extracting reliable exponents of $\ln L$ is not possible (especially with logarithmic corrections to scaling) the fact that the *coefficients* and ratios between these—extracted several ways—are in reasonable agreement is a more stringent test. But even if the random force equivalence is *not* valid, the data of Fig. 3 clearly indicate the instability of large systems to dislocation pairs. Note that this is true for arbitrarily weak randomness: as shown in [5] weak randomness is equivalent to large dislocation core energy, but this will be overcome by the $-(\ln L)^{3/2}$ for large L. Widely spaced dislocations will thus proliferate driving the elastic constant K to zero and destroying the order [8,15].

We conclude with an alternate picture of the elastic glass, developed for the three-dimensional case [5]. The basic excitations from a ground state are fractal domain walls surrounding regions in which h changes by b. Their fractal dimension, d_w, will be the same as that for the forced open wall that connects a pair of dislocations [Fig. 1(c)]: $d_w^{\text{fixed-pairs}} = 1.28(3) \approx d_w^{\text{optimized-pairs}} = 1.30(3)$. The energy of a scale L wall constrained only on scale L should vary by $O((\ln L)^{1/2})$ but have mean independent of L. The incoherent logarithmic sum over scales yields for the fixed-end open domain wall energy, both mean and variations of order $\ln L$—as we found. But if the end positions can adjust to lower the wall energy near the dislocation at each scale, the energies add up *coherently* resulting in the $-(\ln L)^{3/2}$ mean optimal dislocation pair energy with order $(\ln L)^{1/2}$ variations dominated by the largest scale, in an analogous way to the extrema of the $g(\mathbf{r})$ of the random force picture. Since the defect energy is concentrated on the domain wall, while it is spread out over a region of area $O(L^2)$ in the random force approximation, it is surprising that these yield the same predictions. But the fact that our results agree well with the domain wall picture in 2D lends strong support to the validity of the analogous picture in the 3D case for which it has been used to conclude that the 3D elastic glass phase is stable to dislocation loops [5].

We thank J. Kondev and C. L. Henley for useful discussions. This work has been supported in part by the National Science Foundation via Grants No. DMR 9630064, No. DMS 9304586, and Harvard University No. MRSEC.

[1] G. Blatter *et al.*, Rev. Mod. Phys. **66**, 1125 (1994).
[2] See, e.g., G. Grüner, Rev. Mod. Phys. **60**, 1129 (1988).
[3] A. I. Larkin and Yu. N. Ovchinikov, J. Low Temp. Phys. **34**, 409 (1979); M. Aizenman and J. Wehr, Phys. Rev. Lett. **62**, 2503 (1989).
[4] T. Giamarchi and P. Le Doussal, Phys. Rev. Lett. **72**, 1530 (1994); Phys. Rev. B **52**, 1242 (1995); M. Gingras and D. A. Huse, Phys. Rev. B **53**, 15 193 (1996); J. Kierfeld, T. Natterman, and T. Hwa, Phys. Rev. B **55**, 626 (1997), and references therein.
[5] D. S. Fisher, Phys. Rev. Lett. **78**, 1964 (1997).
[6] H. W. J. Blöte and B. Nienhuis, Phys. Rev. Lett. **72**, 1372 (1994); J. Kondev *et al.*, J. Phys. A **29**, 6489 (1996).
[7] C. Zeng, A. A. Middleton, and Y. Shapir, Phys. Rev. Lett. **77**, 3204 (1996).
[8] C. Zeng and P. L. Leath, cond-mat/9810154, 1998.
[9] First argued by J. Villain and J. Fernandez, Z. Phys. B **54**, 139 (1984).
[10] See e.g., J. L. Cardy and S. Ostlund, Phys. Rev. B **25**, 6899 (1982); J. Toner and D. P. DiVincenzo, Phys. Rev. B **41**, 632 (1990); T. Hwa and D. S. Fisher, Phys. Rev. Lett. **72**, 2466 (1994).
[11] See, e.g., M. P. A. Fisher, P. Weichman, G. Grinstein, and D. S. Fisher, Phys. Rev. B **40**, 546 (1989).
[12] D. Carpentier and P. Le Doussal, Phys. Rev. B **55**, 12 128 (1997).
[13] A related analysis is performed in B. Derrida, Phys. Rev. B **24**, 2613 (1981); B. Derrida and H. Spohn, J. Stat. Phys. **51**, 817 (1988); see also Appendix of D. S. Fisher and D. A. Huse, Phys. Rev. B **43**, 10 728 (1991).
[14] For $\alpha = 0$, a similar hierarchical argument was used to obtain $A = \sqrt{8/\pi}$; D. Carpentier and P. Le Doussal, Phys. Rev. Lett. **81**, 2558 (1998).
[15] A. A. Middleton, cond-mat/9807374, 1998.